Journal of Thermal Analysis and Calorimetry, Vol. 84 (2006) 2, 483–487

THERMAL ANALYSIS OF PREALLOYED Fe–3Cr–0.5Mo SINTERED STEEL

*M. Campos**, *L. Blanco and J. M. Torralba*

Departamento of Materials Science and Engineering, Universidad Carlos III de Madrid, Avenida de la Universidad, 30. 28911 Leganés, Spain

Thermal analysis was done to determine the temperatures of thermal reactions, phase transformations or melting reaction during continuous heating. These reactions are a direct response to the steel composition and to the sintering atmosphere. Simultaneous thermal analysis TG-DTA (STA) shows up the sintering behaviour of sintered low prealloyed chromium steels and their peculiarities. Given the high oxygen affinity of chromium, graphite additions can modify their thermal reactions, and hence the sintering behaviour of the steel. Evidence is given of the effect of carbon on the sintering process and the nature of the oxides.

Keywords: *Cr–Mo low-alloyed sintered steels, DTA, simultaneous thermal analysis (STA), TG*

Introduction

Cr and Mo are widely used as alloying elements in conventional ingot steels for heat treatments, but the peculiarities of Cr for sintering restricted its use in powder metallurgy (PM) during the 60s to the research labs [1, 2]. Low Cr alloyed steels possess however, all the requirements for most structural components and for the new needs of the market [3].

In the mid 80's, work was begun with low chromium content prealloyed powders, water or oil atomised [4, 5]. These first experiments were related to innovating the processing conditions and used a well-defined selected dew point to avoid oxidation during sintering. But in spite of the demand for high performance materials, industry was not ready for the particularities of these materials. Additional advantages of chromium as an alloying element of PM steels are its low cost and good recyclability as compared with copper. These alloys can be used directly as scrap in the conventional pig iron industry [6, 7].

Together with chromium and molybdenum, nickel is the third alloying element most used in the conventional steel industry, and was one of the elements most often used in the PM industry of steels. Nickel can be recycled as scrap, but since it was classified as a dangerous substance by the European Union [8, 9], several studies and investigations have been made in Europe, aimed to substitute nickel in the PM industry by new families of nickel free alloys with high performance.

This stimulates research and development of chromium low-alloyed steels process by PM, and the first step is by thermal analysis. Since the reactions produced in the material by a thermal process are a response to the applied atmosphere and to its composition, thermal and chemical analyses are effective in disclosing the dependence of material properties upon temperature. Thermal analysis results provided to Gojic the information to determinate the tempering stages and critical temperatures in a comparable cast alloy system [10].

As reported in [11] the particle surface oxides are more strongly bonded to the metal so the complete reduction of these oxides can be expected at higher temperatures. In addition, although chromium is in an alloyed state, it remains sensitive to oxidation during sintering and also during the cooling process. But as proposed by [12] an appropriate control of oxygen partial pressure during the sintering cycle can lead to mechanical properties comparable to those of Cu–Ni–Mo alloyed materials.

Experimental

Experiments using different atmospheres and admixed carbon were performed with low-alloyed chromium–molybdenum steel. The effect of hydrogen as a reducing agent is investigated by using different atmospheres in the tests, i.e., an inert atmosphere (Ar) and one that can be used for the sintering operation ($90N_2$–$10H_2$–$0.1CH_4$). In earlier studies, Lindberg [13] showed that at 1120°C and in this atmosphere, a partial oxygen pressure of $>10^{-18}$ atm is enough to oxidise the chromium, so the dew point must be kept below –26°C.

A first report of the role of carbon in these steels [14], reducing the importance of the atmosphere, gave

* Author for correspondence: campos@ing.uc3m.es

1388–6150/$20.00

Akadémiai Kiadó, Budapest, Hungary
Springer, Dordrecht, The Netherlands

admixed carbon as the reducing agent. So considering all the sources of oxygen, the oxide surface particles must first be reduced to favour diffusion and avoid this critical partial pressure of oxygen which would lead to oxygen enrichment.

Specimens were uniaxially compacted at 700 MPa, from fully prealloyed water-atomised powders of the composition detailed in Table 1 (Astaloy CrM grade, from Höganäs AB, Sweden). To test the role of graphite additions, samples were prepared carbon free and with three different graphite amounts: 0.2–0.35 and 0.5 mass%.

Table 1 Chemical analysis of supplied powders

C	<0.01
O_{tot}	<0.25
Cr	3.00
Mo	0.50
Fe	bal

The evolution of the powders during the sintering cycle was studied by STA, recording simultaneously DTA and TG curves, in a Neztech unit. These tests measure the mass change and the reactions of the mixtures. The test was performed in controlled atmosphere, up to 1550°C, to reach the melting point of the alloy, with a heating and cooling rate of 7°C min^{-1}. Samples are pressed better than loose powder to decrease the exposed surface and to reproduce the sintering conditions, keeping their masses between 150 and 200 mg. The sample and the reference material (pure alumina powder) were placed in pure alumina crucibles (Fig. 1).

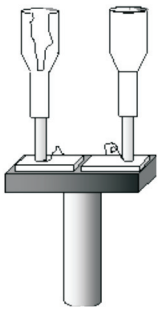

Fig. 1 STA crucibles

Since the changes of mass and of enthalpy run parallel, the combination of the two graphs (DTA and TG) shows the distinction between the phase transition and the oxidation. The phase transitions are shown by a peak in the DTA graph without any associated change of mass in the TG curve. But although it is theoretically possible to distinguish between the oxidation (exothermic peak) and a phase transition (endothermic peak in the heating stage and exothermic during cooling), this is difficult in practice because the process of oxidation is continuous and the inertia of the system during the heating does not provide a good base line, so the distinction between the reactions is not clear in the DTA curves [15–17]. During the heating step, the heat sources surround the specimens, whereas during cooling there is only one source of heat, i.e., the specimen. During cooling, the heat goes from inside the sample to outside, so the recorded peaks depend on thermal conductivity of the specimen, considering also the porosity. For this reason, the phase transitions are studied in the cooling stage.

The evolution of oxygen, nitrogen and combined carbon content, obtained by chemical analysis using a Leco TC 136 (for oxygen) and a Leco CS 200 (for combined carbon), is contrasted with reactions detected by thermal analysis.

Results and discussion

To compare, locate and interpret the reactions correctly, a control test was made on an iron standard sample in Ar (Fig. 2). On the DTA curve, during heating, two peaks correspond to α→γ and γ→δ transitions (at 909 and 1380°C, respectively) and a third one is that of the melting point of the iron (1515°C). During cooling, the solidification is the first peak (1471°C) followed by the other two transition reactions at slightly lower temperatures (at 1370 and 883°C) [18].

The same test with the Fe–3Cr–0.5Mo alloy carbon free (Fig. 3) showed that the gradual increase of mass shown in the TG can be associated with a process of oxidisation that starts (according to the peaks of the DTA curve) around 350°C. As the temperature rises, endothermic peaks indicate the phase transformation at 893, 1350 and melting at 1522°C (the last endothermic peak) [18]. Chromium and molybdenum decrease the γ-field and increase the temperature range of δ-Fe.

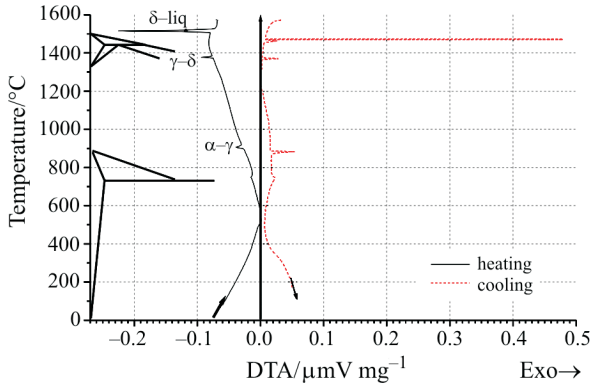

Fig. 2 Iron standard STA, in argon. Peaks during heating: up to 909°C α→γ; up to 1380°C γ→δ transformation, melting up to 1515°C. Peaks during cooling: solidification 1471°C, up to 1370°C δ→γ and up to 883°C γ→α

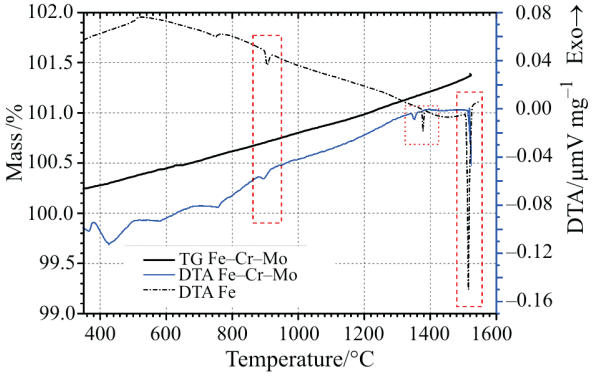

Fig. 3 STA, under Ar, of the prealloyed steel Fe–3Cr–0.5Mo without graphite additions, pressed up to 700 MPa, compared with Fe

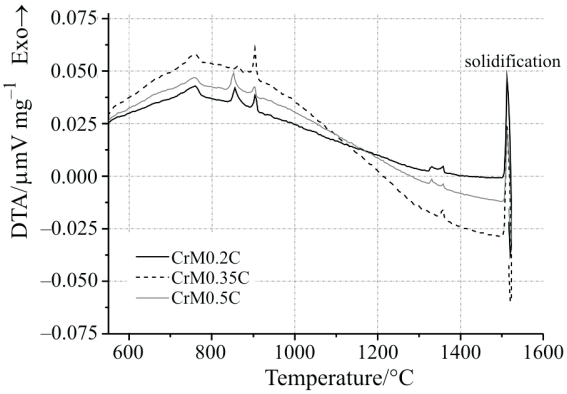

Fig. 5 DTA curves of prealloyed steel with different amounts of graphite additions during cooling step; Ar atmosphere

By using argon atmosphere the effect of additions of graphite as a reducing agent is well defined (Fig. 4). In the carbon-free alloyed steel, the mass shows a steady increase with temperature, which means that even argon atmosphere had sufficient partial pressure of oxygen to oxidise the samples. The presence of graphite causes the arrest of this oxidation at around 1020°C, which means that the carbon is acting as a reducing agent in the course of the sintering process. Unless graphite addition is sufficient, the oxidation will progress at higher temperatures, as it is shown material with 0.35% of graphite addition, which up to 1200°C is oxidised again.

Figure 5 shows the results of the differential thermal analysis (DTA) performed with various additions of graphite to an Fe–3Cr–0.5Mo alloy in Ar atmosphere. The curves of cooling are used here since the peaks – all exothermic in this case – are more clearly defined. All the results from Fig. 5 are in coherence with the work of Yu [19] who determined the constitution of the phase diagram of this alloyed steel, applying thermodynamic calculation with the Thermo-Calc programme [20]. The low carbon content of the eutectoid should be noted, and the different 2-phase fields that would be crossed during a heating-cooling process. Following the analysis with the help of Fig. 5 and starting from the right, the point of solidification is the first peak (at around 1520°C); then the peritectic reaction, following with three peaks. As in the phase diagram proposed by Yu [19], the first one agrees with the solvus line of the 2-phase field $\alpha+\gamma$, the next is the eutectoid reaction, and the last one another solvus line of the carbide $M_{23}C_6$ field. After solidification, the mass continues to increase, and the exothermic peaks correspond to the phase transitions (with no associated change of mass) [18]. At around 928°C, linked to a change in the increase of mass, an exothermic peak records a reaction of oxidation. This shows that the steel may still be subjected to oxidation during cooling.

When an atmosphere of $90N_2+10H_2+0.1CH_4$ is used, two reducing agents must now be considered: the hydrogen in the atmosphere and the graphite in the mixture. Again the partial pressure of oxygen is high enough to cause oxidation, as is seen in the TG curves (Fig. 6). The question now is whether in this atmosphere of $90N_2+10H_2$ and in spite of the oxygen in the atmosphere, the reduction effected by the

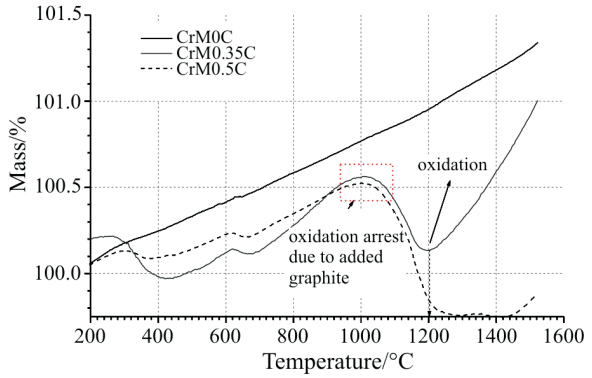

Fig. 4 Prealloyed steel TG depending on different amount of graphite admixed; Ar atmosphere

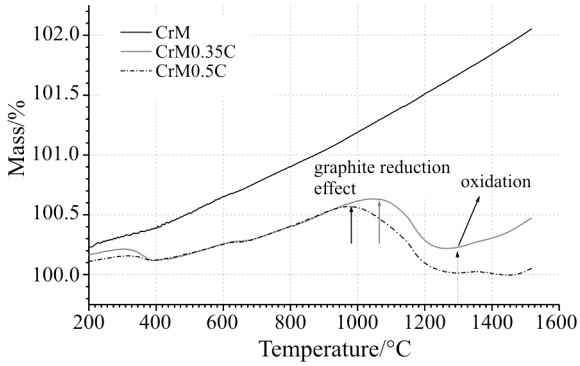

Fig. 6 TG curves of prealloyed Fe–3Cr–0.5Mo+0, 0.35, 0.5% C in $90N_2–10H_2–0.1CH_4$ atmosphere

Table 2 Oxygen and carbon content once samples have been sintered and cooled at 0.25 and 0.04°C s^{-1}

Sintering conditions	$C_{admixed}$/%	Cooling rate				
		0.25°C s^{-1}		0.04°C s^{-1}		
		$C_{combined}$/%	O/%	$C_{combined}$/%	O/%	N/%
1120°C 30 min	0.2	0.21	0.52	0.28	0.29	0.089
	0.35	0.35	0.28	0.36	0.22	0.087
	0.5	0.49	0.58	0.47	0.19	0.069
1250°C 60 min	0.2	0.18	0.12	0.13	0.02	0.071
	0.35	0.25	0.07	0.28	0.01	0.063
	0.5	0.38	0.03	0.44	0.01	0.052

graphite is sufficient to prevent the oxidation of the chromium during the sintering of the alloy Fe–3Cr–0.5Mo. This can be analysed in Fig. 6. The mass increases shown in the TG curves are a clear indication of the effect of graphite additions. With this atmosphere, the amount of added graphite has a different effect on the evolution of the system. With 0.35% C, oxidation continues up to about 1080°C, and on reaching 1280°C the oxidation of the steel starts again (when this should be in phase γ). By increasing the addition to 0.5% C, it is possible to arrest the oxidation at around 980°C, and, as seen in the curve, no other mass increase occurs with the rise in temperature. It would appear, then, that the combined effect of atmosphere and of the right graphite content improves the behaviour of the material.

Figure 7 gives the results of the differential thermal analysis (DTA) as the amount of graphite added to the prealloyed powder is modified. Reading from right to left, Fig. 7 shows the point of solidification, this time at a lower temperature (about 1507°C). Later, on crossing 2-phase fields, the same peaks of the transition phases and solvus lines are detected at lower temperatures (by some tens of degrees) than in the Ar atmosphere.

To assess the oxidation and the decarburation of the samples, the carbon and oxygen contents must be measured after the sintering process. These first analyses reveal that the greatest losses of carbon are accompanied by a considerable reduction in the amount of oxygen. This was observed in samples sintered at 1250°C, while those sintered at 1120°C showed only a slight decarburation and the oxygen content remained high (Table 2). This suggests that the reduction of oxygen in the samples is more effective at 1250°C and is mainly due to the carbon in the sample rather than to the hydrogen in the atmosphere. The microstructures of etched samples show a total absence of surface decarburization. This uniformity of carbon loss supports the idea of carbon as reducing agent.

Measurements of nitrogen after sintering reject nitrification of the material in spite of the high affinity of chromium with this element. In the faster cooled samples, their oxygen content was higher, and lower the $C_{combined}$ (Table 2). Independently of the final microstructure, this modifies the behaviour of the mechanical properties. At 1120°C, since the reduction was incomplete, the oxide layer on the surface of the particles inhibits diffusion and this weakens their contact.

Sintered microstructures of prealloyed steels with 0.5% of graphite additions shown a good diffusion process between particles, as their initial morphology of powder is erased (Fig. 8).

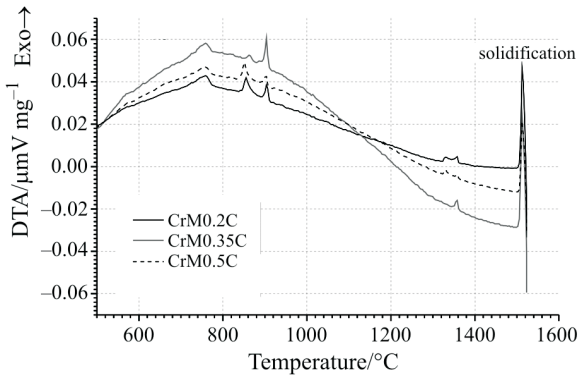

Fig. 7 Prealloyed Fe–3Cr–0.5Mo DTA traces with several graphite additions, during cooling step in $90N_2$–$10H_2$–$0.1CH_4$

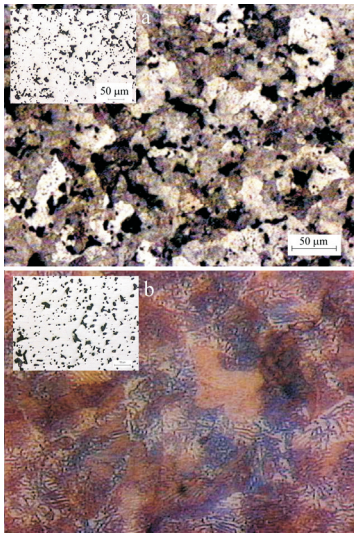

Fig. 8 Etched specimens sintered up to 1250°C, 0.5% $C_{admixed}$, 30 min, 0.04°C min^{-1}; a – 1120, b – 1250°C

Conclusions

STA experiments with a low-alloy Cr–Mo sintered steel have demonstrated the role of carbon as the main reduction agent during the sintering process. Carbon should be added in excess to this alloy system, to provide a self-control of the reduction of oxides, to improve the diffusion rate, the sintering contact and hence the material response. This idea was confirmed by the following:

- The simultaneous thermal analyses (STA) in argon show that carbon acts as the principal reducing agent during the sintering process.
- In tests of $90N_2$–$10H_2$–$0.1CH_4$, the contribution of hydrogen to the reduction process is significant at high temperatures where it prevents new oxidations.
- Even in argon atmosphere, mass increases (oxidation) are observed, although the gains are less than those in tests with $90N_2$–$10H_2$–$0.1CH_4$.
- DTA curves reveal the phase transformation temperatures of this steel. Since the oxygen and carbon contents depend on the sintering atmosphere, this can shift the temperatures.
- The results of chemical analysis of combined oxygen and carbon confirm those of the DTA-TG curves, i.e., that carbon is the main reducing agent during sintering. It is shown that the combined oxygen content is greater with rapid cooling because of the shorter time of reduction. Analysis of nitrogen content reveals that at this pressure and concentration, it is hardly retained in the steel.

Acknowledgements

The Authors thank Höganäs AB, in Sweden, for the financial support of this work through the Höganäs Chair in PM, as well as all the members for their scientific assistance.

References

1 C. G. Goetzel, Treatise on Powder Metallurgy, New York and London Interscience publishers, 1950, Vol. II, pp. 378–407.
2 G. Zapf, G. Hoffmann and K. Dalal, Powder Metall., 18-n°35 (1975) 214.
3 J. M. Torralba and M. Campos, Powder Metall. Progress, 2 (2002) 177.
4 M. Ichidate, I. Karasuno, T. Kubo, K. Koshiro and M. Umino, Horizons Powder Metall., Part II, (1986) 57.
5 Karasumo, K. Koshiro, Masahide Umino and M. Ichidate, Horizons Powder Metall., Part I, (1986) 53.
6 A. Salak, Proc. Int. Conf. Def. Fract. Struct. PM Mat. Stara Lesna. IMR.SAS Kosice, 1996, Vol 1. pp. 209–227.
7 K. Dollmeier, E. Ernst, D. Gonia, M. Holl, J. Wahnschaffe, Conf. Def. Fract. Struct. PM Mat. Stara Lesna. IMR.SAS Kosice, 1996, Vol. 1, pp. 229–241.
8 EC Directive 67/548/EEC.
9 EC Directive 88/379/EEC.
10 M. Gojic, M. Suceska and M. Rajic, J. Therm. Anal. Cal., 75 (2004) 947.
11 M. Campos, S. Kremel and T. Marcu Puscas, Proc. EURO PM'00, Munich, 2000, Vol. 1, pp. 47–54.
12 B. Lindqvist, Proc. Euro PM'00, 2000, Vol. I, pp. 13–21.
13 C. Lindberg, Adv. Powder Metall. Particul. Mater., 13 (1999) 89.
14 H. Danninger, 8th Int. Conf. on Powder Metall. in CSRF, 1992, Vol. 1, pp. 81–91.
15 Robert F. Speyer, Thermal Analysis of Materials, Marcel Dekker, New York 1994.
16 Ferenc Paulik, Special Trends in Thermal Analysis, Wiley and Sons, 1995.
17 M. H. Braga, L. F. Malheiros, J. M. V. Macjado and O. M. Freitas, Proc. Adv. Mater. Process. Techn., 1997, pp. 57–61.
18 M. Campos and J. M. Torralba, Proc. Powder Metall. World Congress, Orlando, USA 2002.
19 Y. Yu, Proc. Powder Metall. World Congress, Kyoto, Japan 2000, Vol. II, pp. 911–914.
20 B. Sundman, B. Jansson and J.-O. Andersson, Calphad, Vol. 9, N° 2 (1985) 153.

Received: July 15, 2005
Accepted: October 26, 2005

DOI: 10.1007/s10973-005-6991-2